Hindawi
Journal of Advanced Transportation
Volume 2020, Article ID 8822117, 12 pages
https://doi.org/10.1155/2020/8822117

Research Article

An Optimal Longitudinal Control Strategy of Platoons Using Improved Particle Swarm Optimization

Zhizhou Wu,[1] Zhibo Gao,[1] Wei Hao,[2,3] and Jiaqi Ma[4]

[1]*The Key Laboratory of Road and Traffic Engineering, Ministry of Education, Tongji University, 4800 Cao'an Road, Jiading, Shanghai 201804, China*
[2]*College of Transportation Engineering, Changsha University of Science and Technology, Changsha 410114, China*
[3]*Hunan Key Laboratory of Smart Roadway and Cooperative Vehicle-Infrastructure System, Changsha University of Science and Technology, Changsha 410004, China*
[4]*Department of Civil and Architectural Engineering and Construction Management, University of Cincinnati, Cincinnati, OH 45221, USA*

Correspondence should be addressed to Zhibo Gao; gaozhibo@tongji.edu.cn

Received 17 June 2020; Revised 3 August 2020; Accepted 29 August 2020; Published 8 September 2020

Academic Editor: Alain Lambert

Most existing longitudinal control strategies for connected and automated vehicles (CAVs) have unclear adaptability without scientific analysis regarding the key parameters of the control algorithm. This paper presents an optimal longitudinal control strategy for a homogeneous CAV platoon. First of all, the CAV platoon models with constant time-headway gap strategy and constant spacing gap strategy were, respectively, established based on the third-order linear vehicle dynamics model. Then, a linear-quadratic optimal controller was designed considering the perspectives of driving safety, efficiency, and ride comfort with three performance indicators including vehicle gap error, relative speed, and desired acceleration. An improved particle swarm optimization algorithm was used to optimize the weighting coefficients for the controller state and control variables. Based on the Matlab/Simulink experimental simulation, the analysis results show that the proposed strategy can significantly reduce the gap error and relative speed and improve the flexibility and initiative of the platoon control strategy compared with the unoptimized strategies. Sensitivity analysis was provided for communication lag and actuator lag in order to prove the applicability and effectiveness of this proposed strategy, which will achieve better distribution of system performance.

1. Introduction

With the development of the urbanization process, traffic demand and the number of motor vehicles have been greatly increased, and the contradiction between traffic supply and demand has become more and more serious, leading to a series of social problems, such as traffic congestion [1, 2], environmental pollution [3, 4], accident frequency [5–8], and energy waste [9, 10]. With the advantages of information acquisition, perception, response time, and interaction behavior, connected and automated vehicles (CAVs) are expected to improve the traffic flow characteristics from the microlevel, thus providing an effective method to solve problems such as traffic congestion and traffic safety [11–13]. Adaptive cruise control (ACC) is an important technology in CAVs longitudinal control and ACC vehicles can obtain the real-time status information (position, speed, acceleration, etc.) of the preceding vehicle through on-board detection equipment with the acceleration optimization algorithm to maintain the constant gap for the preceding vehicle [14]. As a more complex form of ACC system, cooperative adaptive cruise control (CACC) vehicles can actively communicate with the preceding vehicle through vehicle-to-vehicle (V2V) communication technology to coordinate their speed changes to form platoons that allow them to follow the preceding vehicles safely with short gaps [15]. A successful CACC operation strategy can increase the probability of making individual CACC vehicles join the platoons. Once a

CAV platoon is formed, the strategy can also help maintain the platoon operation throughout a highway corridor. However, there are many factors affecting the application effect for the CACC system, among which the most critical ones are spacing strategy and control algorithm. Before the implementation of large-scale field real vehicle test, it is necessary to study the influence of different spacing strategies and control algorithms on the performance of CACC system in order to improve the theory of CACC system and promote the promotion of its technology.

During the process of vehicle longitudinal control, the reasonable spacing control strategy is one of the keys to ensuring high safety, car-following stability, and satisfactory road capacity. In recent years, a variety of control strategies have been put forward, which are mainly divided into constant spacing gap (CSG) strategy, constant time-headway gap (CTG) strategy, and variable time-headway gap (VTG) strategy. CSG strategy shows that the vehicle always maintains a constant intervehicle distance with the preceding vehicle [16, 17]. Due to its simple structure and low application difficulty, it is first applied in highway environment with relatively little interference [18]. However, CSG strategy is insensitive to the change of vehicle speed and has poor adaptability to the platoon stability in the complex and changeable driving environment. In order to deal with these shortcomings, some strategies in which the gap varies with the driving environment are proposed, such as CTG strategy and VTG strategy. CTG strategy refers to the constant time headway between the subject vehicle and the preceding vehicle by constantly adjusting the speed under the car-following state [19]. With further research, the flexibility and stability of CTG strategy, like CSG strategy, cannot meet the requirements of the complex traffic system [20]. Therefore, some VTG strategies that the time headway can change with the traffic flow environment have attracted the attention of researchers. With due consideration of the influence of vehicle speed, acceleration, and relative speed changes by varied time headway, Yanakiev and Kanellakopoulos [21] presented a variable headway strategy and proved that the proposed strategy can guarantee platoon stability. In addition, some variable time-headway strategies were proposed for different driving behaviors, such as perception, judgment, and operation [22, 23].

In the car-following mode, it is greatly necessary to take into consideration various factors such as comfort, safety, car-following stability, traffic capacity, and energy consumption except considering a stable safety control strategy between the vehicle and the preceding vehicle. From the perspective of optimal control, the design of a reasonable and effective control algorithm is another research hotspot of CACC system design. The design of a reasonable and effective control algorithm from the perspective of optimal control is another focus of CACC research field. Presently, the theories and methods applied to the car-following mode of CACC system include classical proportional integral differential (PID) control, model predictive control (MPC), and artificial neural network and linear-quadratic (LQ) control. For the nonlinear characteristics of CACC system, PID is applied to realize the automatic adjustment of the performance index parameters [24]. Through control strategies such as prediction model, rolling optimization, and feedback correction, MPC can take into account multiple control objectives and constraints simultaneously, which is conducive to meeting multiple control requirements during vehicle driving [25]. The disadvantage of MPC is that the model structure is too complex. The methods of artificial intelligence mainly include fuzzy control and artificial neural network. The idea is to establish the relationship between input (vehicle position, velocity, acceleration, etc.) and output (desired acceleration, angle, etc.) through the sample training method. It has the advantages of simple design structure, mature algorithm application conditions, and low hardware requirements, and the disadvantages of the model structure are difficult to describe. LQ algorithm, also known as a linear-quadratic algorithm, is an optimal control law based on quadratic performance indexes to obtain state linear feedback and realize closed-loop optimal control. Its advantages are not limited by the concrete model structure and its design is flexible. The disadvantage is that the control performance depends on the weight matrix of state variables and input variables, and these choices are subjective and lack objective description.

To attain optimal gains for PID or LQ algorithm, a series of intelligent optimization algorithms were used, such as Genetic Algorithm (GA) and particle swarm optimization (PSO) methods. Compared with GA and other optimization methods, PSO memorizes satisfactory solutions among all the particles without considering previous knowledge after each evolution, so that it attracts increasing attention for solving complex optimization problems. Sowjanya and Srinivas [26] presented the development of an optimal PID controller for a composition control system using PSO technique. Chen et al. [27] used dynamic particle swarm optimization to develop optimal strategies for two-variable energy management and gear-shifting in hybrid electric vehicles. The results demonstrate that, compared with the baseline case, the proposed optimization strategy brought superior performance when applied to hybrid energy management and transmission control. Rahman et al. [28] investigated the use of the accelerated particle swarm optimization (APSO) method for developing real-time and large-scale optimizations for allocating power. Compared with standard particle swarm optimization considering charging time and battery capacity, the APSO method can achieve some improvements in terms of best fitness and computation time. The above studies have revealed that PSO is a reliable tool for designing an optimal strategy and that it can outperform other evolutionary algorithms [27].

The longitudinal control strategy of CAV platoon is complex, especially with the uncertainty of key parameters, and there is a need to develop computationally efficient algorithms to find optimal solutions. The objective of this paper is to design an optimal controller considering the key parameter selection involved in the longitudinal vehicle dynamics. The optimal control is designed by considering the parametric uncertainties in the dynamics model of platoons expressed by a third-order linear vehicle model.

The optimal platooning is then formulated as a linear-quadratic optimal control problem, where optimal desired accelerations are generated to minimize the cost function. The optimal controller regulates platoon desired accelerations to minimize the cost function representing safety, efficiency, and comfort, subject to speed limits, acceleration range, and minimal spacing. In addition, an improved particle swarm optimization (IPSO) algorithm is used to optimize the weighting coefficients for the state variables and input variables. The designed control strategy is flexible in such a way that it can be applied to the homogeneous platooning control with constant time-headway gap and constant spacing gap.

The remainder of this paper is structured as follows. Section 2 introduces the system models for constant time-headway and constant spacing gap platoons with CAVs. Section 3 presents a linear-quadratic optimal controller with an improved particle swarm optimization algorithm. Section 4 designs simulation experiments to verify the performance of the proposed controller and discusses the simulation results of the CAV platoons under different control strategies. Finally, conclusions and recommendations are delivered in Section 5.

2. Dynamics Models

First of all, a single CAV dynamics model is introduced, and then the CAV platoon dynamics models under the strategy of constant time-headway and constant spacing gap are established.

2.1. Single-Vehicle Dynamics Model. In the dynamics modeling process with a single vehicle, it is assumed that a vehicle travels on the road, with l_n, x_n, v_n, and a_n denoting the vehicle length, location, speed, and acceleration of the subject vehicle. According to the second law of Newton's kinematics, the dynamic equation of a single vehicle is listed as follows:

$$\left\{ m_n \cdot \ddot{x}_n = F_n - R_{g,n} - R_{d,n} - R_{a,n}, R_{a,n} = K_{a,n} \cdot \dot{x}_n^2, \right. \quad (1)$$

where m_n denotes the mass of vehicle n, F_n denotes the driving force produced by vehicle's engine, $R_{g,n}$, $R_{d,n}$, and $R_{a,n}$ denote the grade resistance, mechanical drag, and aerodynamic drag, respectively, and $K_{a,n}$ denotes the aerodynamic drag coefficient.

The vehicle engine model can be considered as a first-order lag system as expressed by [29]

$$\dot{F}_n = -\frac{F_n}{\tau^A} + \frac{U_n}{\tau^A}, \quad (2)$$

where τ^A denotes the vehicle engine time coefficient, U_n denotes the throttle command input, and $U_n \geq 0$ and $U_n \leq 0$ represent power input and brake input, respectively.

Utilizing the feedback linearization control law [30], the nonlinear model in equation (1) can be linearized as a first-order lag system as expressed by

$$\begin{aligned} U_n &= m_n u_n + 2K_{a,n}\dot{x}_n\ddot{x}_n\tau^A + \left(R_{g,n} + R_{d,n} + R_{a,n}\right), \\ \ddot{x}_n &= \frac{1}{\tau^A} \cdot (u_n - x_n), \end{aligned} \quad (3)$$

where u_n denotes the desired acceleration given to vehicle n.

Under the strategy of the constant time-headway gap, the control objective is to keep the speed of the subject vehicle consistent with the preceding and maintain a constant time headway; that is, $s_n^d = v_n \cdot t^d + s_0$, where s_n^d is the desired gap, t^d is the desired time headway, and s_0 is the minimum gap at standstill. For a single vehicle n, the system state is described by the gap error, relative speed to the preceding vehicle, and actual acceleration; that is, $\mathbf{Z} = (\Delta s_n, \Delta v_n, a_n)^T$; and the control variable is defined as $\mathbf{U} = u_n$. Δs_n is the deviation between the real space gap $s_n = x_{n-1} - x_n - l_n$ and the desired gap s_n^d to the preceding vehicle; that is, $\Delta s_n = s_n - s_n^d$. Δv_n is the relative speed to the preceding vehicle.

According to the previous definition of system state and control variable, a third-order model is used to express the longitudinal dynamics model for vehicle n as shown in [31]

$$\frac{\mathrm{d}}{\mathrm{d}t}\mathbf{Z} = \frac{\mathrm{d}}{\mathrm{d}t}(\Delta s_n, \Delta v_n, a_n)^T = \frac{\mathrm{d}}{\mathrm{d}t}\begin{pmatrix} x_{n-1} - x_n - l_n - s_n^d \\ v_{n-1} - v_n \\ a_n \end{pmatrix} = \begin{pmatrix} v_{n-1} - v_n - a_n \cdot t^d \\ a_{n-1} - a_n \\ \dfrac{(u_n - a_n)}{\tau^A} \end{pmatrix}, \quad (4)$$

$$\mathbf{f}(\mathbf{Z}, \mathbf{U}, \mathbf{d}) = \mathbf{A} \cdot \mathbf{Z} + \mathbf{B} \cdot \mathbf{U} + \mathbf{C} \cdot \mathbf{d}, \quad (5)$$

where $\mathbf{A} = \begin{bmatrix} 0 & 1 & -t^d \\ 0 & 0 & -1 \\ 0 & 0 & -1/\tau^A \end{bmatrix}$, $\mathbf{B} = \begin{bmatrix} 0 \\ 0 \\ -1/\tau_n \end{bmatrix}$, $\mathbf{C} = \begin{bmatrix} 0 \\ 1 \\ 0 \end{bmatrix}$, $\mathbf{d} = [a_{n-1}]$, and $\mathbf{d}$ is the external disturbance of the system, which refers to the actual acceleration of the preceding vehicle $n-1$ in this paper.

Under the strategy of the constant spacing gap, the control objective is to maintain a desired space gap between

the subject vehicle n and the preceding vehicle $n-1$; this is $s_n^d = L_d$, where L_d is the desired spacing gap. Compared with the CTG strategy, the change of the CSG strategy is the expression adjustment of gap error; that is, $\Delta s_n = x_{n-1} - x_n - l_n - L_d$. Therefore, the single dynamics model of CSG strategy can still be expressed by equations (4) and (5), and it only needs to set $t^d = 0$.

2.2. Platoon Dynamics Models. For a homogeneous CAV platoon system with $N \geq 2$ vehicles, the system state variables can be defined as $\mathbf{Z}^p = (\Delta s_1, \Delta v_1, a_1, \Delta s_2, \Delta v_2, a_2, \ldots, \Delta s_N, \Delta v_N, a_N)^T$, the control variable can be defined as $\mathbf{U}^p = (u_1, u_2, \ldots, u_N)^T$, and the disturbance can be defined as $\mathbf{d}^p = \mathbf{a}_p$, where $\mathbf{a}_p$ is the actual acceleration of the preceding vehicle $n-1$. For each homogeneous CAV vehicle in this platoon system, it is applicable to the single-vehicle dynamics model. Therefore, the matrix-form system dynamics model for homogeneous CAV platoon can be expressed with

$$\begin{aligned} \frac{\mathrm{d}}{\mathrm{d}t}\mathbf{Z}^p &= \frac{\mathrm{d}}{\mathrm{d}t}(\Delta s_1, \Delta v_1, a_1, \Delta s_2, \Delta v_2, a_2, \ldots, \Delta s_N, \Delta v_N, a_N)^T = g(\mathbf{Z}^p, \mathbf{U}^p, \mathbf{d}^p), \\ g(\mathbf{Z}^p, \mathbf{U}^p, \mathbf{d}^p) &= \mathbf{A}^p \cdot \mathbf{Z}^p + \mathbf{B}^p \cdot \mathbf{U}^p + \mathbf{C}^p \cdot \mathbf{d}^p, \end{aligned} \tag{6}$$

where

$$\begin{aligned} \mathbf{A}^p &= \begin{bmatrix} \mathbf{A}_1^{3\times3} & 0^{3\times3} & \cdots & 0^{3\times3} \\ 0^{3\times3} & \mathbf{A}_2^{3\times4} & \cdots & 0^{3\times3} \\ \vdots & \vdots & \ddots & \vdots \\ 0^{3\times2} & 0^{3\times3} & \cdots & \mathbf{A}_N^{3\times4} \end{bmatrix}, \\ \mathbf{B}^p &= \begin{bmatrix} \mathbf{B}_1 & & 0 \\ & \ddots & \\ 0 & & \mathbf{B}_N \end{bmatrix}, \\ \mathbf{C}^p &= \begin{bmatrix} \mathbf{C} & 0 \\ 0 & 0 \end{bmatrix}, \\ \mathbf{A}_1^{3\times3} &= \begin{bmatrix} 0 & 1 & -t^d \\ 0 & 0 & -1 \\ 0 & 0 & -\left(\frac{1}{\tau^A}\right) \end{bmatrix}, \\ \mathbf{A}_i^{3\times4} &= \begin{bmatrix} 0 & 0 & 1 & -t^d \\ 1 & 0 & 0 & -1 \\ 0 & 0 & 0 & -\left(\frac{1}{\tau^A}\right) \end{bmatrix}, \quad i = 2, 3, \ldots, N, \\ \mathbf{B}_k &= \begin{bmatrix} 0 \\ 0 \\ \frac{1}{\tau^A} \end{bmatrix}, \quad k = 1, 2, \ldots, N. \end{aligned} \tag{7}$$

3. Design of Optimal Controller for Platoon Operation

In this section, a linear-quadratic optimal controller is developed to determine the control command by minimizing a running cost function.

3.1. Platooning Control Formulation. The centralized control method is adopted in the controller design of the CAV platoon, where all the follower information is collected and computed by the leader of a CAV platoon, and then the desired accelerations are broadcast to the followers. Since the platoon dynamics model is linear, a linear-quadratic optimal controller is designed to optimize the performance of CAV platoon operation. The target is to enable the platoon to obtain better performance in terms of driving safety, efficiency, and ride comfort, which is to reduce the gap error, relative speed, and desired acceleration reflecting physical quantity [31]. The controller is used to comprehensively consider each performance indicator through the weighting coefficients. The cost function J is shown in

$$J = \min_{U^p} \int_{t_0}^{t_0+T_p} L(\mathbf{Z}^p(t), \mathbf{U}^p(t))\mathrm{d}t, \tag{8}$$

$$L = c_1 \sum_{i=1}^{N} (\Delta s_i)^2 + c_2 \sum_{i=1}^{N} (\Delta v_i)^2 + c_3 \sum_{i=1}^{N} (u_i)^2. \tag{9}$$

In equation (9), c_1, c_2, and c_3 denote the weighting coefficients of vehicle gap error, relative speed, and desired acceleration, respectively, and $[t_0, t_0 + T_p]$ denotes a time horizon.

In addition to the target performance indicator, the state and control variables in the system should also be constrained. The existing constraints are listed as follows:

(1) Speed constraint:

$$\underline{v} \le v_i \le \overline{v}. \tag{10}$$

(2) Gap constraint:

$$x_i - x_{i+1} \ge s_0 + l_i. \tag{11}$$

(3) Acceleration constraint:

$$\underline{a} \le u_i \le \overline{a}. \tag{12}$$

(4) Other constraints: since the accurate feedback information on vehicle positions, speeds, and actual acceleration is obtained via on-board sensors and V2V communication. The received state at time t_0 is actually measured at time $t_0 - \tau^s$. It is formulated as follows:

$$\widetilde{\mathbf{Z}}^p(t_0) = \mathbf{Z}^p(t_0 - \tau^s), \tag{13}$$

where $\underline{v}$, $\overline{v}$, $\underline{a}$, and $\overline{a}$ denote the lower and upper bounds of the speed and acceleration, respectively, and τ^s is the feedback delay in communication.

In order to facilitate later expression and calculation, the cost function is adjusted to matrix forms, and the expression is listed as follows:

$$J = \min_{U^P\left[t_0, t_0+T_p\right]} \int_{t_0}^{t_0+T_p} \left[\left(\mathbf{Z}^p\right)^T \mathbf{Q} \mathbf{Z}^p + \left(\mathbf{U}^p\right)^T \mathbf{R} \mathbf{U}^p \right] \mathrm{d}t, \tag{14}$$

where

$$\begin{aligned}
\mathbf{Q} &= \begin{bmatrix} \mathbf{q}_1 & & 0^{3\times3} \\ & \ddots & \\ 0^{3\times3} & & \mathbf{q}_i \end{bmatrix}, \\
\mathbf{R} &= \begin{pmatrix} \mathbf{r}_1 & & 0 \\ & \ddots & \\ 0 & & \mathbf{r}_i \end{pmatrix}, \\
\mathbf{q}_i &= \begin{pmatrix} c_1 & 0 & 0 \\ 0 & c_2 & 0 \\ 0 & 0 & 0 \end{pmatrix}, \\
\mathbf{r}_i &= \left[c_3\right]_{1\times1}, \\
i &= 1, 2, \ldots, N.
\end{aligned} \tag{15}$$

The desired acceleration of platoon system can be calculated by

$$\mathbf{U}^p(t) = -\mathbf{K} \cdot \mathbf{Z}^p(t), \tag{16}$$

where $\mathbf{K}$ is the optimal control feedback gain matrix. When the vehicle parameter value and the weighting coefficient value are determined, $\mathbf{K}$ can be obtained by solving Riccati equation:

$$\mathbf{P}\mathbf{A}^p + \left(\mathbf{A}^p\right)^T \mathbf{P} - \mathbf{P}\mathbf{B}^p \mathbf{R}^{-1} \left(\mathbf{B}^p\right)^T \mathbf{P} + \mathbf{Q} = 0, \tag{17}$$

where $\mathbf{P}$ is the solution of Riccati equation (17).

Lastly, the optimal control feedback gain matrix is obtained; that is, $\mathbf{K} = \mathbf{R}^{-1}(\mathbf{B}^p)^T\mathbf{P}$.

3.2. Parameters Optimization. In equations (9) and (14)–(17), it can be seen that the target performance of the system completely depends on the selection of the weighting coefficients c_1, c_2, and c_3. In previous designs, the weighted coefficient is usually obtained by repeated trials, which makes the optimal control law lack theory and objectivity. In this section, an improved particle swarm optimization algorithm is adopted to optimize the weighting coefficients for the controller.

PSO is an intelligent optimization algorithm based on the predation behavior of birds, which has the characteristics of swarm optimization. However, the basic PSO algorithm is prone to fall into local optimization and has a slow convergence rate. Therefore, an IPSO algorithm is introduced to optimize the weight coefficient of the controller. The idea is to use the nonlinear function sigmoid to dynamically adjust the inertia factor, and the algorithm can achieve a good balance in the global space and local space [32]. In the optimization process, the velocity and position of particles in the search space are determined according to the following improved iterative updating formula:

$$\vartheta_{t+1} = \omega_t \vartheta_t + \eta_1 \gamma_1 (P_t - \chi_t) + \eta_2 \gamma_2 (G_t - \chi_t), \tag{18}$$

$$\chi_{t+1} = \chi_t + \vartheta_{t+1}, \tag{19}$$

$$\omega_t = \mathrm{sigmoid}\left(\alpha \cdot \frac{\Delta J}{\vartheta_t}\right), \tag{20}$$

where χ denotes the position of the particle, ϑ denotes the velocity of the particle, ω_t denotes the inertia factor, η_1 and η_2 denote accelerated constant, γ_1 and γ_2 denote a random number between [0, 1], P_t denotes the best position that the particle has searched so far, G_t denotes the best location of the whole particle swarm so far, α denotes the linear change coefficient, and ΔJ denotes the change of fitness function value.

The procedure of controller parameter optimization using IPSO is shown in Figure 1, and the flow of the IPSO algorithm is as follows:

Step 1. Initialize the particle swarm. The positions χ_t and velocities ϑ_t of all particles are generated randomly, and P_t and G_t are determined.

Step 2. Calculate the fitness value of each particle and compare its fitness value with the fitness value of the optimal position P_t experienced by the particle. If it is good, take it as the current P_t.

Step 3. For each particle, compare its fitness value with the fitness value of the optimal position G_t experienced by the whole particle swarm. If it is good, take it as the current G_t.

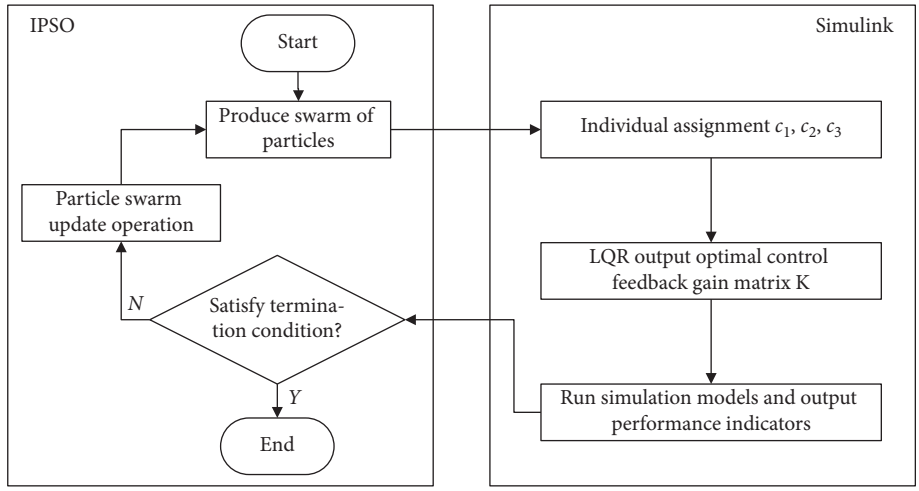

Figure 1: The procedure of controller parameters optimization.

Step 4. Update the velocity and position of particles according to equations (18)–(20).

Step 5. If the termination condition (the maximum number of iterations or the lower limit of the adaptive value) is not met, then return to step (2); otherwise, exit the algorithm and output the optimal solution.

4. Simulation Experimental Design

4.1. Simulation Scenarios. In order to verify the effectiveness of the proposed method, a homogeneous CAV platoon system with $N = 4$ vehicles is selected for this case study, which followed an exogenous head vehicle, as shown in Figure 2. V2V communication is adopted between each following CAV. For convenience, all vehicle lengths, the desired headway, and the minimum gap at standstill are the same.

4.2. Results Analysis. To verify the benefits of the optimal controller of platoons using IPSO, some different strategies were adopted to conduct the comparison:

CTG strategy: desired time headway $t^d = 1$ s [33] and weighting coefficient $c_1 = 0.6$, $c_2 = 0.5$, and $c_3 = 0.6$ [31]

CSG strategy: desired time headway $t^d = 0$ s, desired space gap $L_d = 75$ m, and weighting coefficient $c_1 = 0.6$, $c_2 = 0.5$, and $c_3 = 0.6$

CTG-IPSO strategy: desired time headway $t^d = 1$ s and the weighting coefficient value space is [0.1, 100]

CSG-IPSO strategy: desired time headway $t^d = 0$ s, desired space gap $L_d = 75$ m, and the weighting coefficient value space is [0.1, 100]

During the simulation experiment, the simulation period is 50 s. A step function is used to describe the acceleration for the exogenous head vehicle, which starts with an initial speed of 25 m/s, decelerates with $-4\,\text{m/s}^2$ from 10 s to 12 s, and then accelerates with $1\,\text{m/s}^2$ from 27 s to 35 s. For other time slots, its acceleration is $0\,\text{m/s}^2$. For the controllers, the parameters are set as follows: $l_i = 4$ m, $s_0 = 2$ m, $L_d = 75$ m, $\tau^A = 0.2$ s, $\tau^s = 0.05$ s, $\underline{v} = 0$ m/s, $\overline{v} = 120/3.6$ m/s, $\underline{a} = -5\,\text{m/s}^2$, and $\overline{a} = 2\,\text{m/s}^2$. For the IPSO algorithm, the parameters are set as follows: $\eta_1 = \eta_1 = 2$, $\alpha = 1$, particle size is 50, and the maximum iteration is 100.

To ensure the stability of the results, the simulations of CTG-IPSO and CSG-IPSO controllers run 10 times, and the optimization procedure is shown in Figure 3. The simulation results of each scheme are shown in Table 1 and Figures 4–7. In Figure 3, the algorithm has converged when the number of iterations is less than 15 generations. This also shows that the controller using the improved particle swarm optimization algorithm has good feasibility. At this time, the weighting coefficients of CTG-IPSO controller are $c_1 = 60.157$, $c_2 = 68.653$, and $c_3 = 0.491$; the total cost is 143.8; the weighting coefficients of CSG-IPSO controller are $c_1 = 5.276$, $c_2 = 100.0$, and $c_3 = 0.295$; and the total cost is 193.0. As depicted in Figures 4–7 and values of costs in Table 1, when the exogenous head vehicle decelerates or accelerates, all controllers give control commands to reduce the relative speeds and gap errors for reducing the costs and settle to a new equilibrium where the cost is zero after a certain time. In addition, the behavior of the first vehicle is more sensitive to the change of the exogenous head vehicle. Since the changes of actual accelerations start from the first vehicle to the last vehicle sequentially, the maximum of absolute relative speed and gap error of the 4th vehicle is smaller than that of the first vehicle. To this end, they can ensure string stability.

In order to describe quantitatively the variation of the performance indicators, the root-mean-square value of performance indicator is analyzed for CAV platoon considering the single CAV performance indicator. The analysis results are shown in Table 2 and Figure 8.

It can be seen from Table 2 that the total cost of the CTG-IPSO controller is decreased by 10.0% compared with the unoptimized CTG controller, wherein the relative speed is reduced by 8.3%, and the actual acceleration is decreased by 3.3% relative to the gap error which increased by 3.0%. In

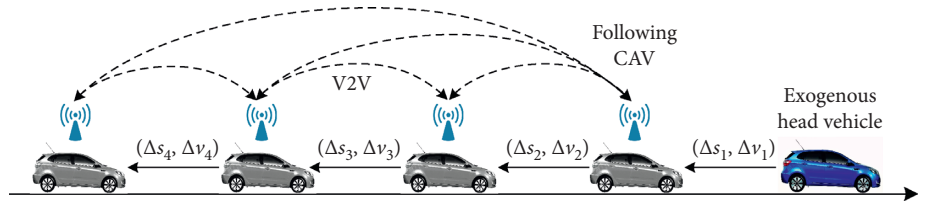

Figure 2: The platooning formations.

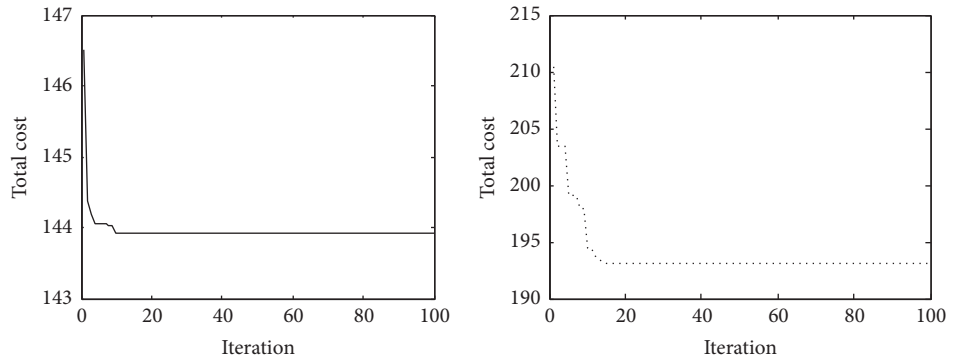

Figure 3: Optimization result of CTG-IPSO scheme and CSG-IPSO scheme: (a) CTG-IPSO and (b) CSG-IPSO.

Table 1: Performance results of platooning controllers.

Indicators	CTG	CSG	CTG-IPSO	CSG-IPSO
$\max \lvert\Delta s_1^+\rvert$ (m)	0.400	2.150	1.132	0.767
$\max \lvert\Delta s_4^+\rvert$ (m)	0.240	0.263	0.247	0.059
$\max \lvert\Delta v_1^+\rvert$ (m/s)	1.037	1.320	1.006	0.295
$\max \lvert\Delta v_4^+\rvert$ (m/s)	0.948	0.152	0.917	0.031
$\max \lvert a_1^+\rvert$ (m/s^2)	1.007	1.179	1.001	1.053
$\max \lvert a_4^+\rvert$ (m/s^2)	0.954	1.265	0.994	1.101
$\min \lvert\Delta s_1^-\rvert$ (m)	0.769	4.638	0.313	1.331
$\min \lvert\Delta s_4^-\rvert$ (m)	0.155	0.504	0.191	0.105
$\min \lvert\Delta v_1^-\rvert$ (m/s)	3.733	2.549	3.057	0.783
$\min \lvert\Delta v_4^-\rvert$ (m/s)	1.417	0.233	1.310	0.070
$\min \lvert a_1^-\rvert$ (m/s^2)	3.553	4.625	3.324	4.205
$\min \lvert a_4^-\rvert$ (m/s^2)	1.447	4.110	1.479	4.392

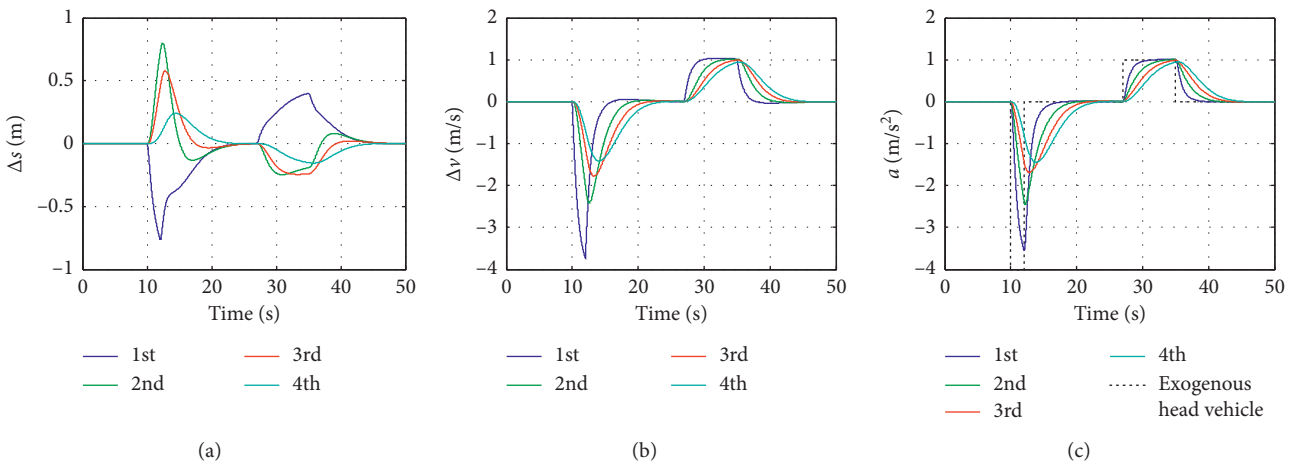

Figure 4: Simulation result of CTG: (a) gap error, (b) relative speed, and (c) acceleration.

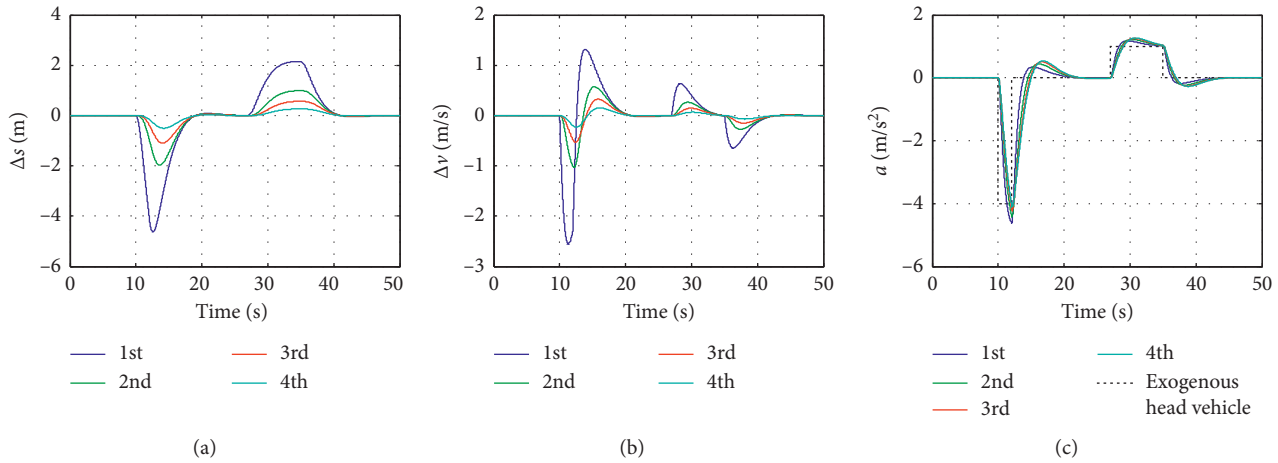

Figure 5: Simulation result of CSG: (a) gap error, (b) relative speed, and (c) actual acceleration.

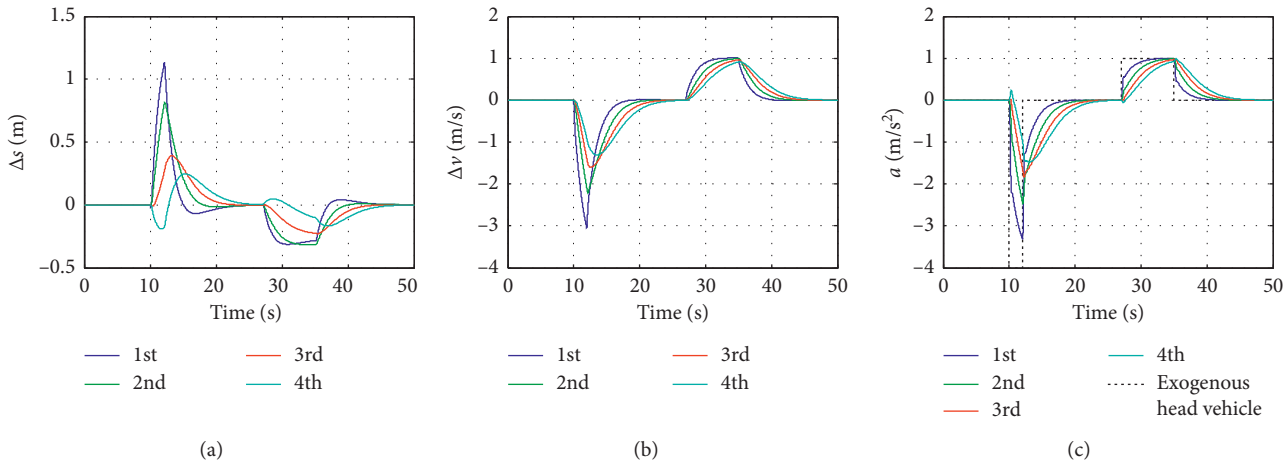

Figure 6: Simulation result of CTG-IPSO: (a) gap error, (b) relative speed, and (c) actual acceleration.

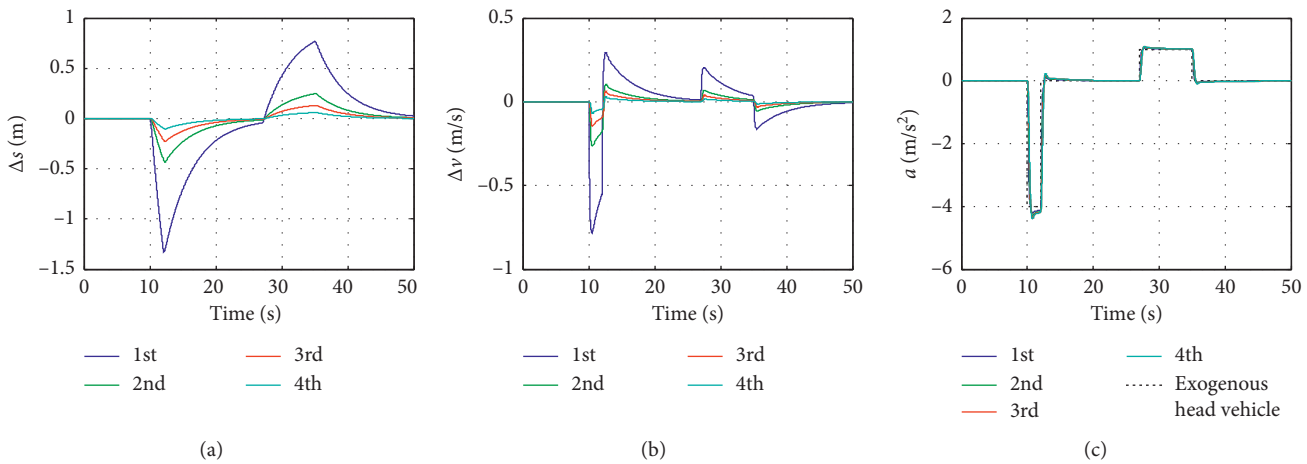

Figure 7: Simulation result of CSG-IPSO: (a) gap error, (b) relative speed, and (c) actual acceleration.

Table 2: The root-mean-square value of performance indicators.

Control strategy	Δs (m)	Δv (m/s)	a (m/s^2)	Total cost
CTG	0.166	0.626	0.612	159.7
CSG	0.735	0.317	0.898	292.7
CTG-IPSO	0.171	0.574	0.592	143.8
CSG-IPSO	0.226	0.085	0.911	193.0

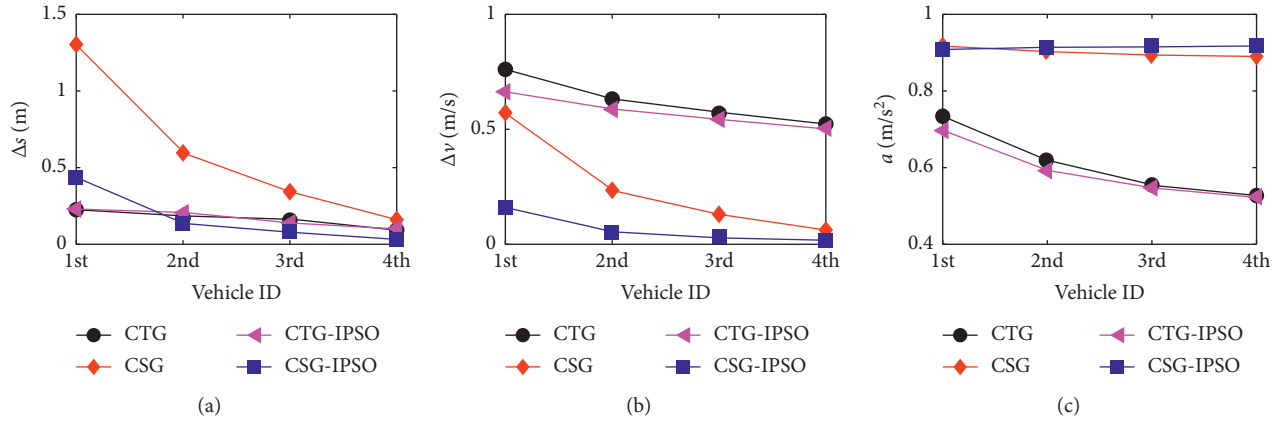

Figure 8: Performance indicator for single CAV: (a) gap error, (b) relative speed, and (c) actual acceleration.

contrast to the unoptimized CSG controller, the total cost of the CSG-IPSO controller decreased by 34.1%, wherein the vehicle gap error decreased by 69.3% and the relative speed decreased by 73.2% combined with the actual acceleration which increased by 1.5%. It can be seen from the changes in total cost and performance that the controller designed in this paper has certain benefits for different control strategies.

As depicted in Figures 8(a) and 8(b), the vehicle gap error and the relative speed for each controller decrease with the increase of the vehicle number order. The decreasing trend of CTG and CTG-IPSO is slow, while the decreasing trend of the CSP and CSP-IPSO controllers is dramatic. It can be seen from Figure 8(c) that the actual acceleration of the CTG and CTG-IPSO controllers decreases sharply with the increase of the number order, but the CTG-IPSO controller is better than CTG. The actual acceleration of the CSG-IPSO and CSG controllers is maintained at 0.9 m/s^2. This is because, under the constant time-headway gap strategy, the desired vehicle spacing is no longer fixed but changes linearly with the change of vehicle speed. At this time, the position and speed information of the leading car are independent of the following car. The subject vehicle only needs to maintain a constant time headway with the preceding vehicle, and it can also maintain the safety and stability of the system with less acceleration.

4.3. Sensitivity Analysis of Key Parameters. Hysteresis is one of the three characteristics of the car-following model and is inevitable in the CACC system. In CACC system, there are mainly two types: communication lag and mechanical lag. In this paper, mechanical lag refers to the time coefficient of the automobile engine, namely, the actuator lag. Therefore, this section mainly analyzes the impact of communication lag and actuator lag on the proposed method.

4.3.1. Communication Lag. With the values of other parameters fixed, the communication lag value varies between 0 s and 0.2 s with an interval of 0.05 s. The optimized system performance indicator and total cost are shown in Tables 3 and 4.

As can be seen from Table 3, with the increase of the communication lag, the vehicle gap error of CTG controller decreases, but the relative speed and actual acceleration increase. Compared with the CTG controller, the CTG-IPSO controller improves the gap error, relative speed, and actual acceleration together with the system total cost which decreases by 8.1%–10.0%. It can be seen from Table 4 that the vehicle gap error, the relative speed, and the actual acceleration of CSG and CSG-IPSO controllers increase with the increase of communication lag. Compared with the CSG controller, the CSG-IPSO controller improves the vehicle gap error and the relative speed, but the actual acceleration is slightly increased combined with the total cost reduced by 22.2%–35.7%. The analysis results show that the controller designed in this paper can improve system efficiency with different communication lag and gap control strategies. In addition, when communication lag increases from 0 s to 0.2 s, the total cost of CTG and CTG-IPSO controllers will be increased by 4.7% and 6.9%, respectively, and the total cost of CSG and CSG-IPSO controllers will be increased by 12.3% and 35.9%, respectively. This finding shows that the constant time-headway gap strategy can overcome the interference caused by communication lag, which is suitable for vehicle formation driving under extreme communication conditions.

Table 3: Sensitivity analysis of communication lag of CTG and CTG-IPSO.

τ^s	CTG				CTG-IPSO			
	Δs (m)	Δv (m/s)	a (m/s^2)	Total cost	Δs (m)	Δv (m/s)	a (m/s^2)	Total cost
0	0.167	0.624	0.608	158.3	0.177	0.572	0.587	142.5
0.05	0.166	0.626	0.612	159.7	0.171	0.574	0.592	143.8
0.10	0.166	0.627	0.617	161.4	0.164	0.577	0.599	146.1
0.15	0.164	0.629	0.623	163.4	0.157	0.581	0.608	148.9
0.20	0.164	0.631	0.627	165.7	0.153	0.585	0.617	152.3

Table 4: Sensitivity analysis of communication lag of CSG and CSG-IPSO.

τ^s	CSG				CSG-IPSO			
	Δs (m)	Δv (m/s)	a (m/s^2)	Total cost	Δs (m)	Δv (m/s)	a (m/s^2)	Total cost
0	0.730	0.310	0.884	285.4	0.187	0.064	0.896	183.5
0.05	0.735	0.317	0.898	292.7	0.226	0.085	0.911	193.0
0.10	0.739	0.325	0.913	300.9	0.287	0.121	0.933	208.2
0.15	0.744	0.334	0.926	310.1	0.361	0.169	0.962	229.1
0.20	0.750	0.344	0.948	320.4	0.416	0.205	0.988	249.4

Table 5: Sensitivity analysis of actuator lag of CTG and CTG-IPSO.

τ^A	CTG				CTG-IPSO			
	Δs (m)	Δv (m/s)	a (m/s^2)	Total cost	Δs (m)	Δv (m/s)	a (m/s^2)	Total cost
0.1	0.147	0.616	0.606	153.9	0.178	0.571	0.590	142.0
0.2	0.166	0.626	0.612	159.7	0.171	0.574	0.592	143.9
0.3	0.189	0.635	0.618	166.4	0.162	0.576	0.595	146.4
0.4	0.214	0.645	0.623	173.7	0.154	0.578	0.597	149.5
0.5	0.241	0.654	0.627	181.6	0.145	0.581	0.599	153.1

Table 6: Sensitivity analysis of actuator lag of CSG and CSG-IPSO.

τ^A	CSG				CSG-IPSO			
	Δs (m)	Δv (m/s)	a (m/s^2)	Total cost	Δs (m)	Δv (m/s)	a (m/s^2)	Total cost
0.1	0.674	0.290	0.886	265.3	0.190	0.068	0.905	177.5
0.2	0.735	0.317	0.898	292.7	0.226	0.085	0.911	193.0
0.3	0.794	0.343	0.907	321.8	0.265	0.102	0.916	211.3
0.4	0.852	0.367	0.913	352.2	0.305	0.120	0.920	231.8
0.5	0.909	0.389	0.917	383.7	0.341	0.134	0.923	254.6

4.3.2. Actuator Lag. With the values of other parameters fixed, the actuator lag value varies between 0.1 s and 0.5 s with an interval of 0.1 s. The optimized system performance indicator and total cost are shown in Tables 5 and 6.

It is shown in Table 5 that the performance indicators of CTG and CTG-IPSO controllers increase with the increase of actuator lag, but the vehicle gap error of CTG-IPSO controller decreases. Compared with the CTG scheme, the CTG-IPSO controller reduces the vehicle gap error, relative speed, and actual acceleration together with the total cost which decreases by 7.7%–15.7%. In addition, it can be seen from Table 6 that the vehicle gap error, relative speed, and actual acceleration of the CSG and CSG-IPSO controllers increased with the increase of the actuator lag. Compared with the CSG controller, the CSG-IPSO controller has improved by the vehicle gap error and the relative speed; however, the actual acceleration is slightly increased combined with the total cost reduced by 33.1%–34.3%. The analysis results also show that the controller designed in this paper can improve the system efficiency with different actuator lag and gap strategies.

In addition, when actuator lag increases from 0.1 s to 0.5 s, the total cost of CTG and CTG-IPSO controllers will be increased by 18.0% and 7.8%, respectively, and the total cost of CSG and CSG-IPSO controllers will be increased by 44.6% and 43.4%, respectively. This finding also shows that the constant time-headway gap strategy can overcome the adverse effects caused by actuator lag and has excellent flexibility and initiative, and it is suitable for vehicle formation driving under extreme mechanical conditions.

5. Conclusions

Most studies have used constant time-headway gap or constant spacing gap as the CACC control strategy, and the weighting coefficients of the performance indicators are calculated

according to subjective judgment in order to achieve the optimal control for the system. However, the strategy type and weighting coefficient uncertainties will directly affect the optimal performance of the system under different driving environments. In this paper, an optimal longitudinal control strategy of platoons using improved particle swarm optimization has been proposed to address these issues. The controlled object in this proposed strategy is the homogeneous platoon model under the constant time-headway strategy and constant spacing strategy. In order to overcome the interference caused by changing the acceleration of the exogenous head vehicle, a linear-quadratic optimal controller is designed with the consideration of the feedback delay and weighting coefficient uncertainties. The controller is optimized by an improved particle swarm optimization algorithm. The simulation results show that the CTG-IPSO controller can reduce the total cost by 10%, vehicle relative speed by 8.3%, and actual acceleration by 3.3% compared with the unoptimized controller. The CSG-IPSO controller can reduce the total cost by 34.1% and reduce the vehicle gap error by 69.3%, reducing the relative speed by 73.2%. Whether it is a constant time-headway gap strategy or constant spacing gap strategy, the strategy proposed in this paper can obtain good control benefits. In addition, the sensitivity analysis of the two parameters, communication lag and actuator lag, further proves the adaptability and effectiveness of the proposed strategy and also reveals that the constant time-headway gap strategy has great flexibility and initiative with the balance of performance indicators, which is applicable to form platoons in extreme conditions.

In order to highlight the benefits of the proposed method, the homogeneous platoon system is chosen as the research object which does not consider the design and optimization of the controller under the heterogeneous traffic flow mixed with CAVs and human-driven vehicles. During the actual complex traffic scenarios, the variable time-headway gap strategy has greater flexibility and adaptability. Therefore, future research should consider the stability analysis and controller design of platoons under the variable time-headway gap strategy. Furthermore, the controller designed in this paper only considers the objectives of safety, efficiency, and comfort. How to introduce the energy consumption for the original basis is also a potential topic which needs to be expanded in the next research.

Data Availability

The data used to support the findings of this study are included within the article.

Conflicts of Interest

The authors declare that there are no conflicts of interest regarding the publication of this paper.

Acknowledgments

This work was supported by the National Natural Science Foundation of China under Grant nos. 61773288 and 51808057 and was supported in part by the National Key Research and Development Program of China (no. 2018YFB1600805).

References

[1] J. Rios-Torres and A. A. Malikopoulos, "A survey on the coordination of connected and automated vehicles at intersections and merging at highway on-ramps," *IEEE Transactions on Intelligent Transportation Systems*, vol. 18, no. 5, pp. 1066–1077, 2017.

[2] C. Yu, Y. Feng, H. X. Liu, W. Ma, and X. Yang, "Integrated optimization of traffic signals and vehicle trajectories at isolated urban intersections," *Transportation Research Part B: Methodological*, vol. 112, pp. 89–112, 2018.

[3] M. Barth and K. Boriboonsomsin, "Real-world carbon dioxide impacts of traffic congestion," *Transportation Research Record*, vol. 2058, no. 1, pp. 163–171, 2008.

[4] N. Jollands, P. Waide, M. Ellis et al., "The 25 IEA energy efficiency policy recommendations to the G8 gleneagles plan of action," *Energy Policy*, vol. 38, no. 11, pp. 6409–6418, 2010.

[5] W. Hao, C. Kamga, X. Yang et al., "Driver injury severity study for truck involved accidents at highway-rail grade crossings in the United States," *Transportation Research Part F: Traffic Psychology and Behaviour*, vol. 43, pp. 379–386, 2016.

[6] Q. Zeng, W. Gu, X. Zhang et al., "Analyzing freeway crash severity using a Bayesian spatial generalized ordered logit model with conditional autoregressive priors," *Accident Analysis & Prevention*, vol. 127, pp. 87–95, 2019.

[7] Q. Wen, H. Wen, H. Huang, and M. Abdel-Aty, "A bayesian spatial random parameters tobit model for analyzing crash rates on roadway segments," *Accident Analysis & Prevention*, vol. 100, pp. 37–43, 2017.

[8] F. Chen and S. Chen, "Injury severities of truck drivers in single- and multi-vehicle accidents on rural highways," *Accident Analysis & Prevention*, vol. 43, no. 5, pp. 1677–1688, 2011.

[9] X. He, H. X. Liu, and X. Liu, "Optimal vehicle speed trajectory on a signalized arterial with consideration of queue," *Transportation Research Part C: Emerging Technologies*, vol. 61, pp. 106–120, 2015.

[10] H. Yang, H. Rakha, and M. V. Ala, "Eco-cooperative adaptive cruise control at signalized intersections considering queue effects," *IEEE Transactions on Intelligent Transportation Systems*, vol. 18, no. 16, pp. 1575–1585, 2016.

[11] L. Xiao, M. Wang, W. Schakel, and B. van Arem, "Unravelling effects of cooperative adaptive cruise control deactivation on traffic flow characteristics at merging bottlenecks," *Transportation Research Part C: Emerging Technologies*, vol. 96, pp. 380–397, 2018.

[12] F. Chen, M. Song, X. Ma, and X. Zhu, "Assess the impacts of different autonomous trucks' lateral control modes on asphalt pavement performance," *Transportation Research Part C: Emerging Technologies*, vol. 103, pp. 17–29, 2019.

[13] Q. Shi and H. Zhuang, "Fault diagnosis of an autonomous vehicle with an improved SVM algorithm subject tounbalanced datasets," *IEEE Transactions on Industrial Electronics*, 2020.

[14] Y. Qin, H. Wang, W. Wang, and D. Ni, "Review of car-following models of adaptive cruise control," *Journal of Traffic and Transportation Engineering*, vol. 17, no. 3, pp. 121–130, 2017.

[15] G. Marsden, M. McDonald, and M. Brackstone, "Towards an understanding of adaptive cruise control," *Transportation*

Research Part C: Emerging Technologies, vol. 9, no. 1, pp. 33–51, 2001.

[16] S. Hoogendoorn, R. Hoogendoorn, M. Wang, and W. Daamen, "Modeling driver, driver support, and cooperative systems with dynamic optimal control," *Transportation Research Record: Journal of the Transportation Research Board*, vol. 2316, no. 1, pp. 20–30, 2012.

[17] D. Swaroop, J. K. Hedrick, C. C. Chien, and P. Ioannou, "A comparision of spacing and headway control laws for automatically controlled vehicles," *Vehicle System Dynamics*, vol. 23, no. 1, pp. 597–625, 1994.

[18] J. Zhou and H. Peng, "Range policy of adaptive cruise control vehicles for improved flow stability and string stability," *IEEE Transactions on Intelligent Transportation Systems*, vol. 6, no. 2, pp. 229–237, 2005.

[19] P. Y. Li and A. Shrivastava, "Traffic flow stability induced by constant time headway policy for adaptive cruise control vehicles," *Transportation Research Part C: Emerging Technologies*, vol. 10, no. 4, pp. 275–301, 2002.

[20] Y. H. Chiang and J. C. Juang, "Longitudinal vehicle control with the spacing policy in consideration of brake input limits," in *Proceedings of the 2007 IEEE International Conference on Systems, Man and Cybernetics*, October 2007.

[21] D. Yanakiev and I. Kanellakopoulos, "Nonlinear spacing policies for automated heavy-duty vehicles," *IEEE Transactions on Vehicular Technology*, vol. 47, no. 4, pp. 1365–1377, 1998.

[22] G. N. Bifulco, L. Pariota, F. Simonelli, and R. Di Pace, "Development and testing of a fully adaptive cruise control system," *Transportation Research Part C: Emerging Technologies*, vol. 29, pp. 156–170, 2013.

[23] A. Rosenfeld, Z. Bareket, C. V. Goldman, D. J. LeBlanc, and O. Tsimhoni, "Learning drivers' behavior to improve adaptive cruise control," *Journal of Intelligent Transportation Systems*, vol. 19, no. 1, pp. 18–31, 2014.

[24] J. Villagra, B. Vinagre, and I. Tejado, "Data-driven fractional PID control: application to DC motors in flexible joints," *IFAC Proceedings Volumes*, vol. 45, no. 3, pp. 709–714, 2012.

[25] L. Luo, *Vehicle Adaptive Cruise Control and the Corresponding Macroscopic Traffic Flow Model*, Zhejiang University, Hangzhou, China, 2011, in Chinese.

[26] K. L. Sowjanya and L. R. Srinivas, "Tuning of PID controllers using particle swarm optimization," *International Journal of Industrial Electronics and Electrical Engineering*, vol. 3, no. 2, pp. 17–22, 2015.

[27] S.-Y. Chen, C.-H. Wu, Y.-H. Hung, and C.-T. Chung, "Optimal strategies of energy management integrated with transmission control for a hybrid electric vehicle using dynamic particle swarm optimization," *Energy*, vol. 160, no. 1, pp. 154–170, 2018.

[28] I. Rahman, P. M. Vasant, B. S. M. Singh, and M. Abdullah-Al-Wadud, "On the performance of accelerated particle swarm optimization for charging plug-in hybrid electric vehicles," *Alexandria Engineering Journal*, vol. 55, no. 1, pp. 419–426, 2016.

[29] M. Wang, "Infrastructure assisted adaptive driving to stabilise heterogeneous vehicle strings," *Transportation Research Part C: Emerging Technologies*, vol. 91, pp. 276–295, 2018.

[30] I. G. Jin and G. Orosz, "Dynamics of connected vehicle systems with delayed acceleration feedback," *Transportation Research Part C: Emerging Technologies*, vol. 46, pp. 46–64, 2014.

[31] N. Chen, M. Wang, T. Alkim, and B. van Arem, "A robust longitudinal control strategy of platoons under model uncertainties and time delays," *Journal of Advanced Transportation*, vol. 2018, Article ID 9852721, 13 pages, 2018.

[32] X. Zhang, Q. Wang, and W. Ji, "An improved particle swarm optimization algorithm for adaptive inertial weights," *Microelectronics & Computer*, vol. 36, no. 3, pp. 66–70, 2019.

[33] L. Xiao and F. Gao, "Practical string stability of platoon of adaptive cruise control vehicles," *IEEE Transactions on Intelligent Transportation Systems*, vol. 12, no. 4, pp. 1184–1194, 2011.